HIF-KDM3A-MMP12 regulatory circuit ensures trophoblast plasticity and placental adaptations to hypoxia

Damayanti Chakraborty[a,b,1], Wei Cui[a,b,2], Gracy X. Rosario[a,b,3], Regan L. Scott[a,b], Pramod Dhakal[a,b], Stephen J. Renaud[a,b,4], Makoto Tachibana[c], M. A. Karim Rumi[a,b], Clifford W. Mason[a,d], Adam J. Krieg[a,d,5], and Michael J. Soares[a,b,d,1]

[a]Institute for Reproductive Health and Regenerative Medicine, University of Kansas Medical Center, Kansas City, KS 66160; [b]Department of Pathology and Laboratory Medicine, University of Kansas Medical Center, Kansas City, KS 66160; [c]Department of Enzyme Chemistry, Institute for Enzyme Research, Tokushima University, Tokushima 770-8503, Japan; and [d]Department of Obstetrics and Gynecology, University of Kansas Medical Center, Kansas City, KS 66160

Edited by R. Michael Roberts, University of Missouri–Columbia, Columbia, MO, and approved October 5, 2016 (received for review July 31, 2016)

The hemochorial placenta develops from the coordinated multilineage differentiation of trophoblast stem (TS) cells. An invasive trophoblast cell lineage remodels uterine spiral arteries, facilitating nutrient flow, failure of which is associated with pathological conditions such as preeclampsia, intrauterine growth restriction, and preterm birth. Hypoxia plays an instructive role in influencing trophoblast cell differentiation and regulating placental organization. Key downstream hypoxia-activated events were delineated using rat TS cells and tested in vivo, using trophoblast-specific lentiviral gene delivery and genome editing. DNA microarray analyses performed on rat TS cells exposed to ambient or low oxygen and pregnant rats exposed to ambient or hypoxic conditions showed up-regulation of genes characteristic of an invasive/vascular remodeling/inflammatory phenotype. Among the shared up-regulated genes was matrix metallopeptidase 12 (MMP12). To explore the functional importance of MMP12 in trophoblast cell-directed spiral artery remodeling, we generated an *Mmp12* mutant rat model using transcription activator-like nucleases-mediated genome editing. Homozygous mutant placentation sites showed decreased hypoxia-dependent endovascular trophoblast invasion and impaired trophoblast-directed spiral artery remodeling. A link was established between hypoxia/HIF and MMP12; however, evidence did not support *Mmp12* as a direct target of HIF action. Lysine demethylase 3A (KDM3A) was identified as mediator of hypoxia/HIF regulation of *Mmp12*. Knockdown of KDM3A in rat TS cells inhibited the expression of a subset of the hypoxia–hypoxia inducible factor (HIF)-dependent transcripts, including *Mmp12*, altered H3K9 methylation status, and decreased hypoxia-induced trophoblast cell invasion in vitro and in vivo. The hypoxia-HIF-KDM3A-MMP12 regulatory circuit is conserved and facilitates placental adaptations to environmental challenges.

placenta | hypoxia | trophoblast invasion | epigenetics | plasticity

Vascular remodeling is an important pregnancy-associated adaptation in hemochorial placentation and is orchestrated, in part, from the contributions of invasive trophoblast cells (also termed extravillous trophoblast) (1–3). These cells invade into the uterus and restructure spiral arteries turning them into flaccid low resistance vessels facilitating the flow of maternal resources to the placenta and then to the fetus. Failure of trophoblast cell invasion and vascular remodeling is associated with pathological conditions such as preeclampsia, intrauterine growth restriction, and preterm birth (3–5). Invasive trophoblast cells arise from trophoblast stem (TS)/progenitor cell populations and can be classified based on their entry into the uterine parenchyma (5, 6). Endovascular invasive trophoblast cells enter uterine spiral arteries, facilitate removal of the endothelium, acquire a pseudovascular phenotype, and restructure the spiral artery, whereas interstitial invasive trophoblast cells migrate into a specialized uterine stroma, termed decidua, and infiltrate areas surrounding the spiral arteries (2, 4, 7, 8). These seminal events in hemochorial placentation are conserved in the rat and human (9–11).

Placentation is a malleable process responsive to a range of stimuli present in the maternal environment (6, 12). As in other tissues, low oxygen is a potent driver of vascular development at the maternal-fetal interface. Hypoxia exposure can redirect placental organization and promote development of the invasive trophoblast cell lineage and uterine spiral artery remodeling, representing adaptive responses conserved in the rat, monkey, and human (13–16). Cellular responses to oxygen deficits are mediated by hypoxia inducible factor (HIF), a transcription factor consisting of a heterodimer composed of oxygen sensitive

Significance

The hemochorial placenta is a dynamic structure endowed with responsibilities controlling the extraction of maternal resources, ensuring fetal development and preserving maternal health. A healthy placenta exhibits plasticity and can adapt to environmental challenges. Such adaptations can be executed through instructive actions on trophoblast stem cells, influencing their abilities to expand and differentiate into specialized cells that accommodate the challenge. Hypoxia, when appropriately timed, promotes invasive trophoblast-directed uterine spiral artery remodeling. Hypoxia activates hypoxia inducible factor-dependent expression of lysine demethylase 3A, modifying the histone landscape on key target genes, including matrix metallopeptidase 12, which acts to facilitate trophoblast invasion and uterine vascular remodeling. Plasticity and adaptations at the maternal–fetal interface safeguard placental development and the healthy progression of pregnancy.

Author contributions: D.C. and M.J.S. designed research; D.C., W.C., G.X.R., R.L.S., and P.D. performed research; M.T. and C.W.M. contributed new reagents/analytic tools; D.C., S.J.R., M.A.K.R., A.J.K., and M.J.S. analyzed data; and D.C. and M.J.S. wrote the paper.

The authors declare no conflict of interest.

This article is a PNAS Direct Submission.

Data deposition: The data reported in this paper have been dposited in the Gene Expression Omnibus (GEO) database, www.ncbi.nlm.nih.gov/geo (accession nos. GSE80339 and GSE80340).

[1]To whom correspondence may be addressed. Email: dchakraborty@kumc.edu or msoares@kumc.edu.

[2]Present address: Department of Veterinary & Animal Sciences, University of Massachusetts, Amherst, MA 01003.

[3]Present address: Department of Biochemistry, Global Pathways Institute, Mumbai 400066, India.

[4]Present address: Department of Anatomy and Cell Biology, University of Western Ontario, London, ON, Canada N6A 3K7.

[5]Present address: Department of Obstetrics and Gynecology, Oregon Health & Science University, Portland, OR 97239.

This article contains supporting information online at www.pnas.org/lookup/suppl/doi:10.1073/pnas.1612626113/-/DCSupplemental.

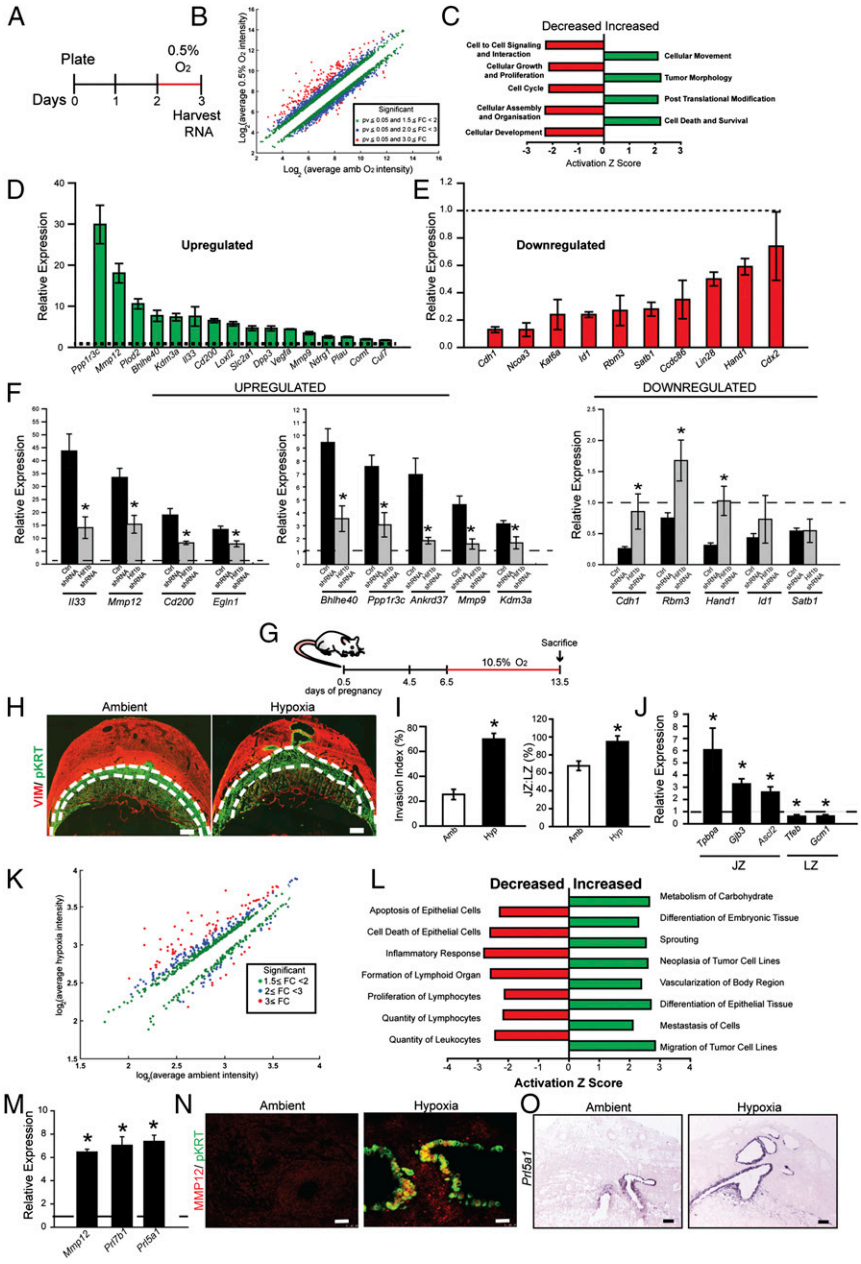

Fig. 1. Hypoxia-dependent responses of TS cells and the placentation site. (*A*) Schematic representation of TS cell exposure to low oxygen tension (0.5% O_2 for 24 h) before harvesting RNA for DNA microarray analysis. (*B*) Scatter plot presentation of in vitro hypoxia-responsive transcripts. (*C*) Presentation of pathway analysis of transcripts differentially expressed following TS cell exposure to 0.5% O_2. (*D* and *E*) Validation of select differentially expressed transcripts by qRT-PCR. All hypoxia responses are significantly different from ambient control (n = 5/group; P < 0.05). (*F*) Examination of the dependence of hypoxia-dependent transcript changes on HIF signaling. TS cells were exposed to 0.5% O_2 in the presence of control (Ctrl) or *Hif1b* shRNAs. RNA was harvested and transcript levels assessed by qRT-PCR (n = 4/group; ANOVA with Student–Newman–Keuls test, *P < 0.05). Dashed lines represent the ambient control values. (*G*) Schematic representation of in vivo maternal exposure to hypoxia (10.5% O_2). (*H*) Representative cross sections of gd 13.5 placentation sites immunostained for vimentin and cytokeratin from pregnant rats exposed to ambient (Amb) or hypoxia (Hyp, 10.5% O_2). The junctional zone (devoid of vimentin staining) is demarcated by the dashed white lines. (Scale bar, 1 mm.) (*I*) Quantification of invasion of trophoblast cells into the uterine mesometrial compartment and ratio of junctional and labyrinth zones (ambient, n = 10; hypoxia, n = 12; *P < 0.05). (*J*) Relative expression of transcripts associated with the junctional zone (JZ) and labyrinth zone (LZ) (n = 8/group, *P < 0.05). Dashed lines represent the ambient control values. (*K*) Scatter plot presentation of maternal hypoxia-responsive transcripts in the metrial gland. (*L*) Presentation of pathway analysis of differentially expressed transcripts in the metrial glands following hypoxia exposure. (*M*) Validation of selected differentially expressed transcripts by qRT-PCR (n = 10/group, *P < 0.05). Dashed lines represent the ambient control values. (*N*) Immunohistochemical analysis of MMP12 and pan cytokeratin (pKRT) staining in tissue sections from pregnant rats exposed to ambient or hypoxia conditions. (Scale bar, 50 μm.) (*O*) In situ hybridization analysis of *Prl5a1* transcripts in placentation sites from pregnant rats exposed to ambient or hypoxia conditions. (Scale bar, 250 μm.) Data presented in *D–F*, *I*, *J*, and *M* were analyzed with Mann–Whitney test.

HIF1A or HIF2A and a constitutively active HIF1B (also known as aryl hydrocarbon receptor nuclear translocator, ARNT) (17, 18). Mouse mutagenesis experiments have demonstrated the importance of key components of the HIF signaling pathway to the regulation of placentation (19–24). HIF acts on targets directly promoting transcription and cellular adaptations to low oxygen and indirectly via modification of the epigenetic landscape (18). Lysine demethylase 3A (KDM3A; also known as JMJD1A) is a hypoxia/HIF responsive histone 3 lysine 9 (H3K9) demethylase implicated in epigenetic regulation of cell differentiation and tissue homeostasis (25, 26). Structural changes associated with tissue plasticity are engineered via activation of matrix metalloproteinases (MMPs) (27, 28). MMPs are responsive to environmental signals and promote the movement of cells through tissue matrices, facilitate structural changes in blood vessel integrity, and contribute to morphogenesis of the placenta (18, 27, 29–31).

Mechanisms underlying the orchestration of placental adaptations and plasticity are not well understood. In this study, we reveal a central and conserved role for HIF-KDM3A-MMP12 signaling in regulating adaptations at the placentation site.

Results

Hypoxia-Dependent Transcript Responses in TS Cells and at the Placentation Site. Hypoxia signaling regulates the development of the invasive trophoblast cell lineage and uterine spiral artery remodeling (13–16). As a first step toward identifying potential adaptive mechanisms downstream of hypoxia exposure, we profiled transcriptomes of rat TS cells (32) exposed to low oxygen and placentation sites from rats exposed to hypoxic conditions using DNA microarray technology (Gene Expression Omnibus repository: GSE80339 and GSE80340; www.ncbi.nlm.nih.gov/geo/).

TS cells maintained in the stem state were exposed to 0.5% oxygen for 24 h, harvested, and profiled. Under these conditions, TS cells are induced to move through extracellular matrices (15). Cell number was not significantly affected by the oxygen tensions investigated (Fig. S1*A*). Low oxygen conditions resulted in robust effects on gene expression: 838 transcripts were down-regulated

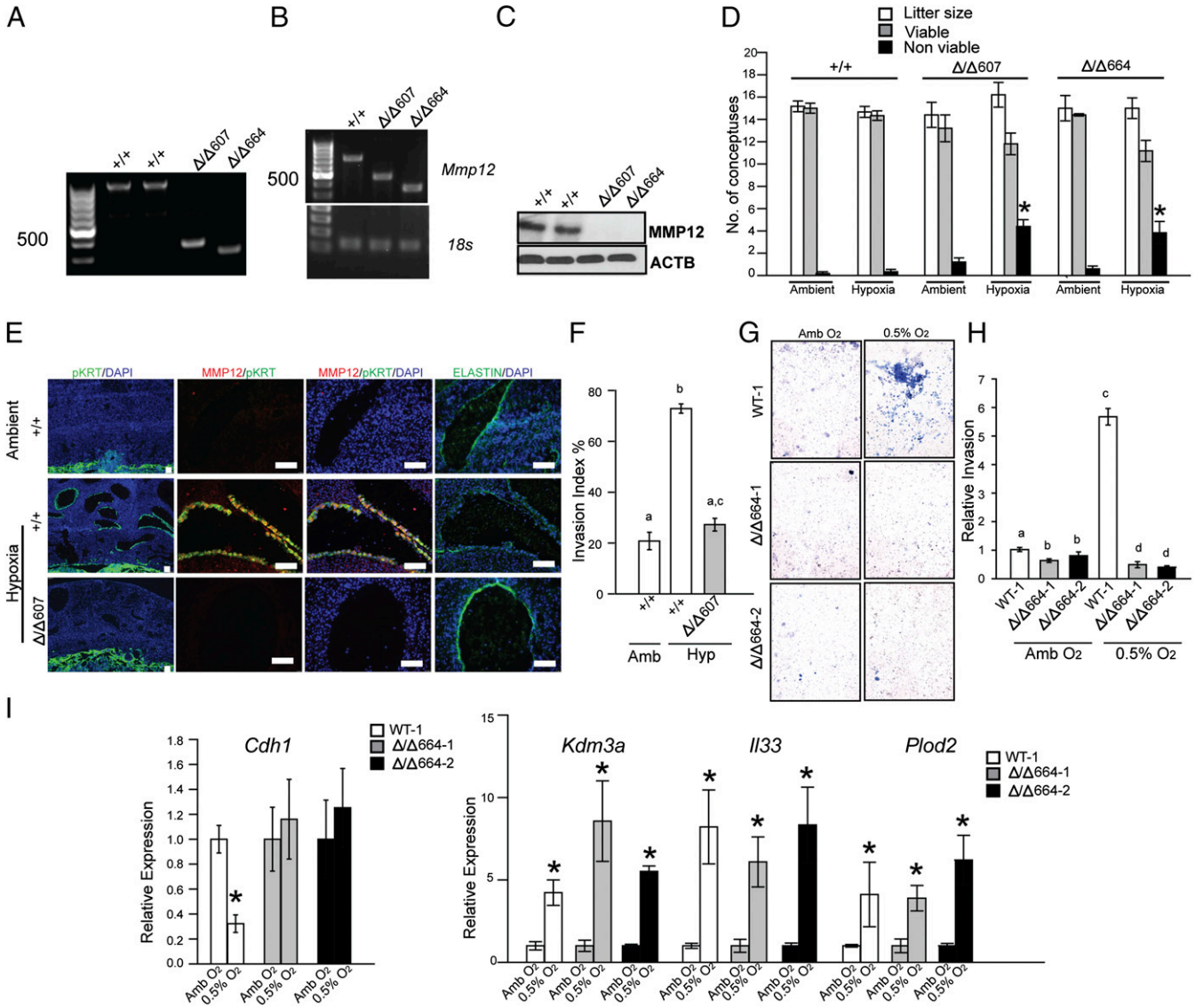

Fig. 2. MMP12 and hypoxia-activated trophoblast-directed uterine spiral artery remodeling. (*A*) Genotyping of WT (+/+) and *Mmp12* homozygous mutant rat strains generated by genome editing. (*B*) RT-PCR analysis for *Mmp12* and *18s* RNAs from spleens of WT (+/+) and *Mmp12* mutant (Δ/Δ607 and Δ/Δ664) rats. (*C*) Western blotting for MMP12 and ACTB from spleens of WT (+/+) and *Mmp12* mutant (Δ/Δ607 and Δ/Δ664) rats. (*D*) Effects of ambient and hypoxia (10.5% O_2) conditions on litter size and the numbers of viable and nonviable conceptuses (+/+, $n = 7$; Δ/Δ 607, $n = 5$; Δ/Δ 664 $n = 5$; $^*P < 0.05$). (*E*) Immunohistochemical analyses (pan cytokeratin, pKRT; MMP12; elastin) of the mesometrial placentation sites from WT (+/+) and *Mmp12* mutant (Δ/Δ607) rats exposed to ambient or hypoxia conditions. (*F*) Quantification of trophoblast cell invasion into the uterine mesometrial compartment. Different letters above bars signify differences among means ($n = 5$/group, $^*P < 0.05$). (*G*) Effects of low oxygen (0.5% O_2) on invasive behavior of WT (WT-1) and two *Mmp12*-null (Δ/Δ664–1 and Δ/Δ664–2) TS cell populations. Images are representative filters. (*H*) Quantification of invasion through Matrigel. Different letters above bars signify differences among means ($n = 5$/group, $P < 0.05$). (*I*) qRT-PCR analysis of hypoxia responsive transcripts in WT (WT-1; white bars) and two *Mmp12*-null (Δ/Δ664–1; gray bars and Δ/Δ664–2; black bars) TS cell populations. Comparisons were between ambient (Amb) and 0.5% O_2 conditions for each genotype ($n = 3$/group, Mann–Whitney test, $^*P < 0.05$). Data presented in *D, F,* and *H* were analyzed with ANOVA and Holm–Sidak (*D*) or Newman–Keuls tests (*F* and *H*).

(≤1.5-fold) and 786 transcripts were up-regulated (≥1.5-fold) in response to low oxygen. Many down-regulated transcripts were associated with the stem state (*Cdh1*, *Cdx2, Bmp4, Id2, Satb1, Rbm3,* and *Lin28*), whereas up-regulated transcripts were characteristic of proteins contributing to cell migration (*Cul7* and *Loxl2*), extracellular matrix remodeling (*Mmp12, Mmp9, Plau, Dpp3,* and *Plod2*), and inflammatory (*Il33* and *Cd200*) phenotypes and adaptive responses to hypoxia (*Egln1, Bhlhe40, Ppp1r3c, Vegfa, Ankrd37,* and *Kdm3a*; Fig. 1 *A–F* and Dataset S1). The involvement of HIF signaling in the transcriptomic responses to hypoxia was evaluated in TS cells expressing HIF1B short hairpin RNAs (shRNAs) or control shRNAs. Down-regulated transcripts showed a mix of HIF dependence, whereas all of the up-regulated transcripts examined were dependent on HIF signaling (Fig. 1*F*). Thus, low oxygen interfered with maintenance of the TS cell stem state and promoted differentiation consistent with an HIF-driven invasive trophoblast cell phenotype.

Because low oxygen promoted TS cell differentiation toward the invasive trophoblast lineage, we sought to identify an in vivo correlate of differentiated invasive trophoblast cells. Hypoxia-exposed gestation day (gd) 13.5 metrial gland tissue contains a prominent population of differentiated invasive endovascular trophoblast cells (14). Rats were exposed to ambient (21% oxygen) or hypoxic environments (10.5% oxygen) from gd 6.5 to 13.5.

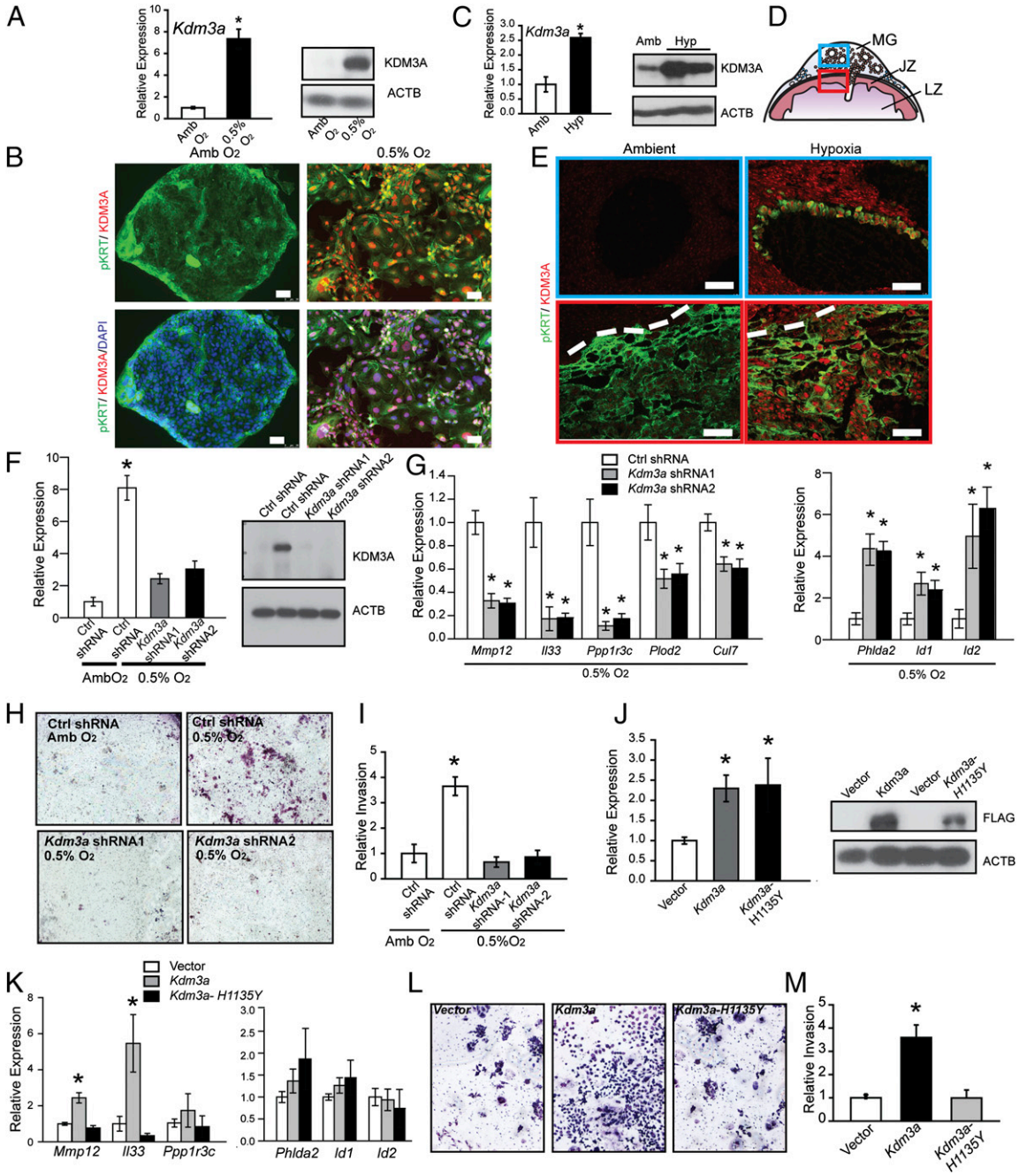

Fig. 3. KDM3A and hypoxia signaling in trophoblast cells. (*A*) *Kdm3a* transcript (qRT-PCR; *Left*) and protein (Western blot; *Right*) responses in TS cells cultured under ambient (Amb) or low oxygen (0.5% O_2). Statistical analysis: $n = 5$/group, Mann–Whitney test, $^*P < 0.05$. (*B*) Immunocytochemical staining for pan-cytokeratin (pKRT) and KDM3A in TS cells cultured under Amb or 0.5% O_2. (Scale bar, 50 μm.) (*C*) In vivo placental *Kdm3a* transcript (qRT-PCR; *Left*) and protein (Western blot; *Right*) responses to maternal hypoxia (10.5% O_2 from gd 6.5 to 13.5). (*D*) Schematic representation of a midgestation placentation site, consisting of the metrial gland (MG), junctional zone (JZ), and labyrinth zone (LZ). The blue box corresponds to the metrial gland region (*Upper*) of *E* and the red box corresponds to the junctional zone (*Lower*) of *E*. (*E*) Immunohistochemistry analysis (pan cytokeratin, pKRT; KDM3A) of gd 13.5 placentation site sections from pregnant rats exposed to ambient and hypoxic conditions. The dashed line in the bottom panels represents the border between the decidua and chorioallantoic placenta. (Scale bar, 100 μm.) (*F*) qRT-PCR and Western blot validation of *Kdm3a* shRNAs. TS cells expressing control (Ctrl) or *Kdm3a* shRNAs were examined in Amb or 0.5% O_2 culture conditions ($n = 4$, $^*P < 0.05$). (*G*) Effects of *Kdm3a* knockdown on hypoxia responsive transcripts in TS cells ($n = 4$, $^*P < 0.05$). (*H*) Effects of Kdm3a knockdown on 0.5% O_2 activated invasive behavior of TS cells. Images are representative filters. (*I*) Quantification of invasion through Matrigel ($n = 3$, Ctrl shRNA + 0.5% O_2 vs. all other treatments, $^*P < 0.05$). (*J*) Ectopic transcript (qRT-PCR; *Left*) and protein (Western blot, *Right*) expression of control (vector) and WT (*Kdm3a*) and mutant (*Kdm3a-H1135Y*) *Kdm3a* constructs stably transfected into TS cells. (*K*) Effects of ectopic expression of control (vector), WT (*Kdm3a*), and mutant *Kdm3a* (*Kdm3a-H1135Y*) constructs stably transfected into TS cells on hypoxia responsive transcripts ($n = 4$, *Kdm3a* vs. vector or *Kdm3a-H1135Y*, $^*P < 0.05$). (*L*) Effects of ectopic expression of control (vector), WT (*Kdm3a*), and mutant *Kdm3a* (*Kdm3a-H1135Y*) constructs stably transfected into TS cells on invasive behavior. Images are representative filters. (*M*) Quantification of invasion through Matrigel ($n = 4$, Kdm3a vs. vector or Kdm3a-H1135Y, $^*P < 0.05$). Data presented in *F, G, I–K*, and *M* were analyzed with ANOVA and Student–Keuls test. ACTB was used as a loading control for the Western blots shown in *A, C, F*, and *J*.

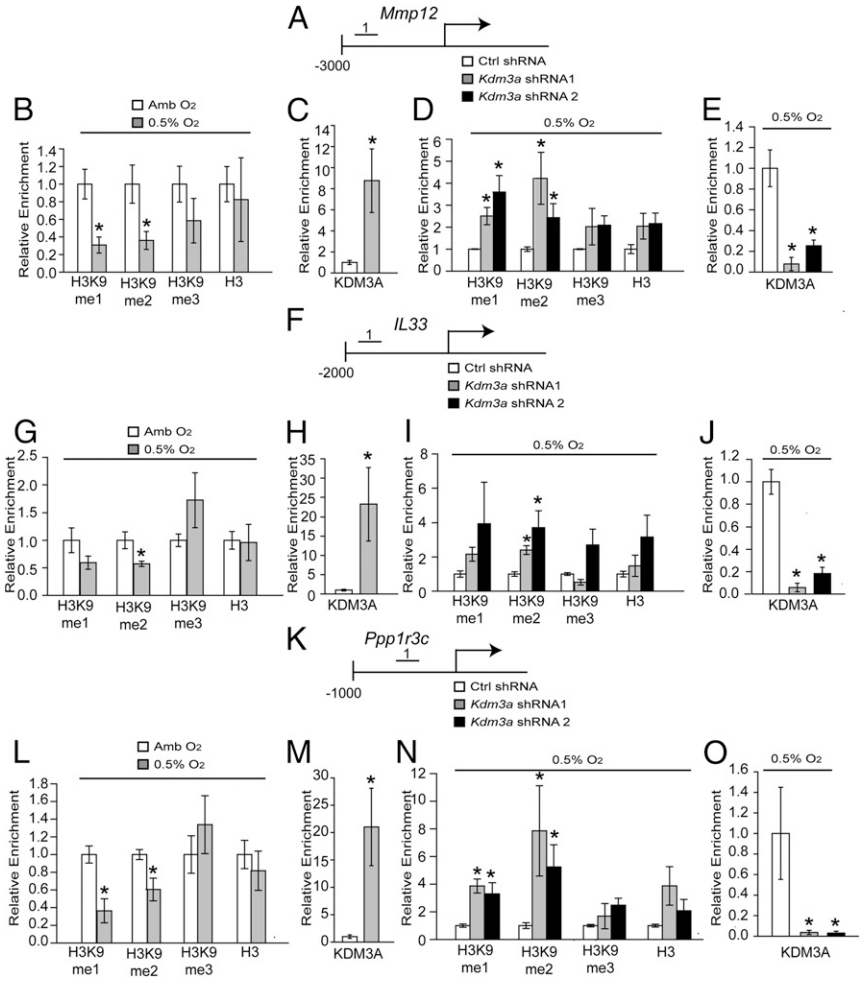

Fig. 4. Histone H3K9 methylation landscape associated with KDM3A targets in hypoxia-exposed TS cells. (*A*) Schematic layout of the rat *Mmp12* gene and the location of one of the regions [No. 1: −2681 to −2568 bp upstream transcription start site (TSS)] surveyed by ChIP analysis in *B–E*. (*B*) ChIP analyses for histone H3K9 methylation (monomethylation, me1; dimethylation, me2; trimethylation, me3) and histone 3 (H3) at the *Mmp12* locus in ambient (Amb) and low oxygen (0.5% O_2) exposed TS cells. (*C*) ChIP analysis for KDM3A at the *Mmp12* locus in Amb and 0.5% O_2 exposed TS cells. (*D*) ChIP analyses for histone H3K9 methylation and H3 at the *Mmp12* locus in 0.5% O_2 exposed TS cells treated with control (Ctrl) or *Kdm3a* shRNAs. (*E*) ChIP analysis for KDM3A at the *Mmp12* locus in 0.5% O_2 exposed TS cells treated with Ctrl or *Kdm3a* shRNAs. (*F*) Schematic layout of the rat *Il33* gene and the location of one of the regions (No. 1: −1372 to −1272 bp upstream of TSS) surveyed by ChIP analysis in *G–J*. (*G*) ChIP analysis for histone H3K9 methylation and H3 at the *Il33* locus in Amb and 0.5% O_2 exposed TS cells. (*H*) ChIP analysis for KDM3A at the *Il33* locus in Amb and 0.5% O_2 exposed TS cells. (*I*) ChIP analyses for histone H3K9 methylation and H3 at the *Il33* locus in 0.5% O_2 exposed TS cells treated with Ctrl or *Kdm3a* shRNAs. (*J*) ChIP analysis for KDM3A at the *Il33* locus in 0.5% O_2 exposed TS cells treated with Ctrl or *Kdm3a* shRNAs. (*K*) Schematic layout of the rat *Ppp1r3c* gene and the location of one of the regions (No. 1: −417 to −316 bp upstream of TSS) surveyed by ChIP analysis in *L–O*. (*L*) ChIP analyses for histone H3K9 methylation and H3 at the *Ppp1r3c* locus in Amb and 0.5% O_2 exposed TS cells. (*M*) ChIP analysis for KDM3A at the *Ppp1r3c* locus in Amb and 0.5% O_2 exposed TS cells. (*N*) ChIP analyses for histone H3K9 methylation and H3 at the *Ppp1r3c* locus in 0.5% O_2 exposed TS cells treated with Ctrl or *Kdm3a* shRNAs. (*O*) ChIP analysis for KDM3A at the *Ppp1r3c* locus in 0.5% O_2 exposed TS cells treated with Ctrl or *Kdm3a* shRNAs. Statistical analyses: $n = 4$; control vs. hypoxia exposed TS cell experiments: Mann–Whitney test, $*P < 0.05$; shRNA experiments: ANOVA with Dunnett's test vs. the control, $*P < 0.05$).

Animals were euthanized at gd 13.5, placentation sites were prepared for assessment of intrauterine trophoblast invasion and spiral artery remodeling or alternatively dissected, and transcript expression was investigated (14, 15). Pregnancy-associated uterine spiral artery remodeling is defined by trophoblast cell intravasation of spiral arteries, their replacement of endothelial cells lining the vessel, and subsequent restructuring the underlying extracellular matrix and dissolution of the tunica media (2, 15). Hypoxia stimulated intrauterine endovascular trophoblast invasion, the preferential allocation of trophoblast cells within the placenta to the junctional zone, and some alterations in the expression of transcripts associated with the junctional zone (*Tpbpa, Gjb3,* and *Ascl2*) and labyrinth zone (*Tfeb* and *Gcm1*; Fig. 1 *G–J*). Transcriptional responses to hypoxia were examined in more detail from the metrial gland (Fig. 1 *K–M*). The metrial gland is a heterogeneous tissue, composed of an assortment or stromal, endothelial, and immune cell populations, and represents the site of intrauterine endovascular trophoblast cell invasion of the spiral arteries (15, 33). A subset of hypoxia-responsive transcripts identified by DNA microarray analysis of the metrial gland exhibited overlap with transcripts up-regulated by low oxygen tension in TS cells, including members of the prolactin family (*Prl5a1* and *Prl7b1*) and MMP12 (Fig. 1*M*, Dataset S1, and Table S1). *Prl5a1* and *Mmp12* expression was restricted to endovascular trophoblast (Fig. 1 *N* and *O* and Fig. S1*B*). MMP12 is a metalloelastase and has been implicated in human trophoblast-directed uterine spiral artery remodeling (30, 34). We used the overlap of in vitro and in vivo profiles and the conservation in rat and human placentation to guide our analysis, which led to a focus on MMP12. In the rat placentation site, MMP12 expression was activated by hypoxia and restricted to invasive endovascular trophoblast cells (Fig. 1*N* and Fig. S1*B*). Thus, MMP12 was viewed as a candidate effector of hypoxia-activated uterine spiral artery remodeling.

MMP12 and Hypoxia-Activated Uterine Spiral Artery Remodeling by Trophoblast Cells. To test the involvement of MMP12 in uterine spiral artery remodeling, *Mmp12* mutant rats were generated using transcription activator-like nucleases (TALEN)-mediated genome editing (Fig. S1 *C–G*). Thirteen founder animals were identified with deletions ranging from 100 to 800 bp. Two deletions encompassing exon 2 (607-bp deletion, referred to as Δ/Δ607; 664-bp deletion, referred to as Δ/Δ664) were further characterized. Each mutation caused nonsense nucleotide frameshifts and premature stop codons, resulting in the interference of MMP12 protein expression, as tested in the spleen and the placentation site (Fig. 2 *A–C*). Heterozygous × heterozygous breeding generated expected Mendelian ratios of progeny genotypes (Fig. S1*F*). *Mmp12*-null × *Mmp12*-null pregnancies yielded modest but significant decreases in litter size and postpartum day 1 neonatal body weights (Fig. S1*G* and Fig. S2*A*). MMP12 deficiency did not adversely affect placentation or intrauterine trophoblast invasion at gd 18.5 (Fig. S2*B*). However, an MMP12 deficit did affect the capacity of the placenta to adapt to hypoxia. WT × WT and *Mmp12*-null × *Mmp12*-null rat mating combinations were challenged with hypoxia (10.5% oxygen) from gd 6.5 to 13.5. Pregnancy outcomes, fetal weights, and intrauterine trophoblast invasion were assessed. *Mmp12*-null pregnancies showed impaired adaptations to hypoxia and significant increases in fetal death (Fig. 2*D*). Disruption of MMP12 expression interfered with

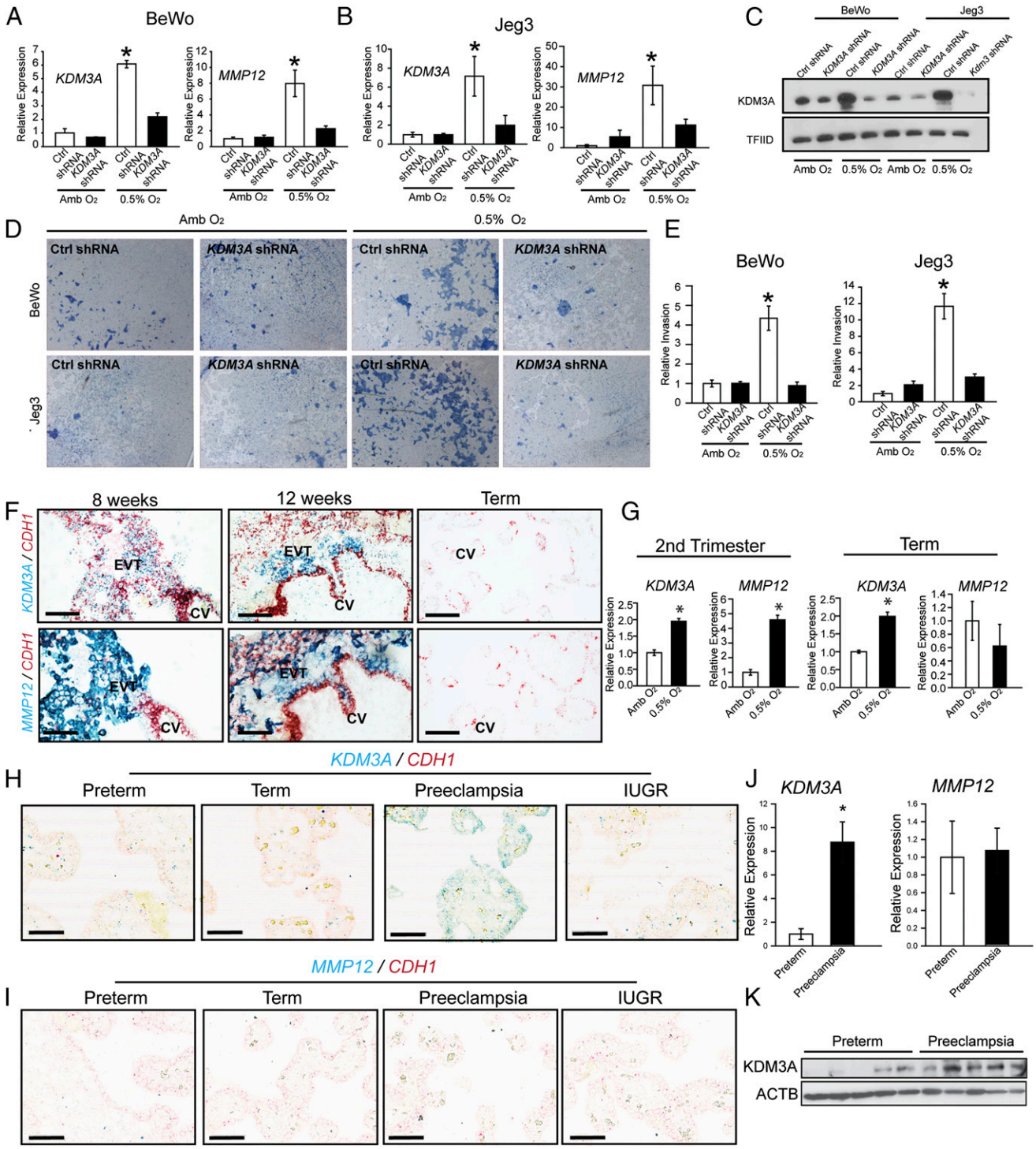

Fig. 5. Conservation of hypoxia-dependent responses in human trophoblast cells. (*A*) Effects of KDM3A knockdown on low oxygen (0.5% O_2) activated *KDM3A* and *MMP12* transcript levels in BeWo human trophoblast cells (qRT-PCR; $n = 3$, $^*P < 0.05$). (*B*) Effects of KDM3A knockdown on 0.5% O_2 activated *KDM3A* and *MMP12* transcript levels in Jeg3 human trophoblast cells (qRT-PCR; $n = 3$, $^*P < 0.05$). (*C*) Effects of KDM3A knockdown on 0.5% O_2 activated KDM3A protein in BeWo and Jeg3 human trophoblast cells. (*D*) Effects of KDM3A knockdown on 0.5% O_2 induced invasive behavior of BeWo and Jeg3 human trophoblast cells. Images are representative *Insets*. (*E*) Quantification of invasion through Matrigel ($n = 3$, $^*P < 0.05$). (*F*) In situ hybridization localization of *CDH1* (red), *KDM3A* (blue, *Top*), and *MMP12* (blue, *Bottom*) transcripts in first trimester (8 and 12 wk) and term human placental tissues. (Scale bar, 100 μm.) CV, chorionic villus; EVT, extravillous trophoblast. (*G*) Second trimester and term primary human trophoblast cell responses to 0.5% O_2. *KDM3A* and *MMP12* transcripts were measured by qRT-PCR (n = 3/group, Student t test, $^*P < 0.001$). (*H*) In situ hybridization localization of *CDH1* (red) and *KDM3A* (blue), transcripts in replicate representative placenta sections from preterm, term, preeclampsia, and intrauterine growth restriction (IUGR) pregnancies (low magnification: scale bar, 300 μm; high magnification: scale bar, 60 μm). (*I*) In situ hybridization localization of *CDH1* (red) and *MMP12* (blue), transcripts in replicate representative placenta sections from preterm, term, preeclampsia, and IUGR pregnancies. (Scale bar, 300 μm.) Data presented in *A*, *B*, and *E* were analyzed with ANOVA and Student–Newman–Keuls test. (*J*) qRT-PCR for *Kdm3a* and *Mmp12* transcripts in placentas from preterm control and preeclamptic pregnancies (n = 6/group, Student t test, $^*P < 0.002$). (*K*) Western blotting for KDM3A protein in placentas from preterm control and preeclamptic pregnancies (n = 5/group).

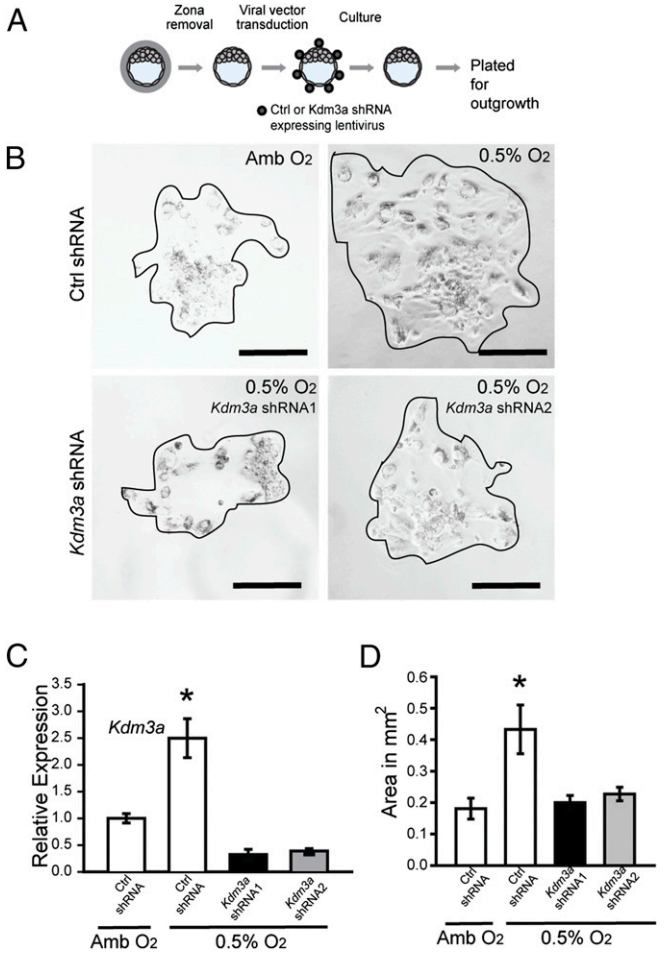

Fig. 6. Effects of oxygen tension and KDM3A expression on blastocyst outgrowth. (*A*) Schematic showing experimental plan for lentiviral transduction of blastocysts and outgrowth assay. Blastocysts were transduced with control (Ctrl) or *Kdm3a* shRNA and cultured for 72 h to allow hatching from the zona pellucida. The attached blastocysts were exposed to ambient (Amb) or low oxygen (0.5% O_2) for 24 h and analyzed. (*B*) Representative images of blastocyst outgrowths from Ctrl shRNA and exposed to Amb, Ctrl shRNA and exposed to 0.5% O_2, and *Kdm3a* shRNAs and exposed to 0.5% O_2. (*C*) Measurement of *Kdm3a* transcripts in control and knockdown cultures was measured by qRT-PCR. Asterisks indicate significant differences among groups (n = 6/group; *$P < 0.05$). (*D*) The bar graph shows quantification of outgrowth area in square millimeters. The area of the outgrowth was measured using Image J software (Ctrl shRNA + Amb, n = 6; Ctrl shRNA + 0.5% O_2, *Kdm3a* shRNA1 + 0.5% O_2, n = 10; *Kdm3a* shRNA2 + 0.5% O_2, n = 10; *$P < 0.05$). Data presented in *C* and *D* were analyzed with ANOVA and Student–Newman–Keuls test.

hypoxia-activated trophoblast invasion and uterine spiral artery remodeling, including impairment of uterine spiral artery-associated elastin degradation (Fig. 2*E*). Similar results were obtained from WT and *Mmp12*-null placentation sites generated from an *Mmp12* heterozygous × *Mmp12* heterozygous breeding scheme (Fig. S2 *C–F*). Shapiro and colleagues noted deficits in *Mmp12*-null mouse macrophage invasive behavior (35), which prompted an evaluation of the direct role of MMP12 on trophoblast cell invasive properties. TS cell lines were established from WT and *Mmp12*-null blastocysts (Fig. S2 *G–I*). Both TS cell populations exhibited FGF4-driven proliferation and mitogen removal-dependent differentiation; however, responses to low oxygen tension differed. Unlike WT TS cells, *Mmp12*-null TS cells showed attenuated low oxygen-activated invasive properties and a failure of *Cdh1* down-regulation when exposed to low oxygen (Fig. 2 *G–I*). Other low oxygen-activated transcriptional behaviors examined did not differ between WT and *Mmp12*-null TS cells (Fig. 2*I*). Collectively, the results indicate that MMP12 is an effector of hypoxia-activated endovascular trophoblast invasion and uterine spiral artery remodeling.

KDM3A and Hypoxia-HIF Signaling in Trophoblast Cells. The above experimentation implicated a link between hypoxia, HIF, and the regulation of MMP12; however, evidence did not support *Mmp12* as a direct target of HIF action. Conserved HIF binding motifs were not present within regulatory DNA associated with the *Mmp12* gene and HIF ChIP sequencing datasets did not support a direct interaction of HIF with the *Mmp12* locus (36–39). Consequently, potential intermediaries were explored. Perusal of the DNA microarray profile generated from TS cells exposed to ambient or low oxygen tension yielded a HIF-dependent candidate mediator, KDM3A (Fig. 1 *D* and *F*). This responsiveness to low oxygen was not shared by two closely related jumonji domain containing family members, *Kdm3b* and *Kdm3c*, or other histone H3K9 demethylases (Fig. S3*A*). KDM3A is a direct target of HIF action in an assortment of cell types (40–43), including TS cells (Fig. 3 *A–E* and Fig. S3 *B–D*), and possesses the capacity to promote gene activation through demethylation of histone H3K9, e.g., removal of a repressive histone mark (25, 26). Accordingly, the involvement of KDM3A in hypoxia-activated trophoblast responses was investigated.

Initially, in vivo responsiveness of KDM3A expression in placentation sites of pregnant rats exposed to normoxic or hypoxic conditions from gd 6.5 to 9.5 or from gd 6.5 to 13.5 was evaluated. At gd 9.5, KDM3A protein was up-regulated by hypoxia at the site of trophoblast progenitors (ectoplacental cone; Fig. S3*E*). KDM3A mRNA and protein were up-regulated at gd 13.5 in endovascular invasive trophoblast and within the junctional zone of hypoxia exposed placentation sites (Fig. 3 *C–E*).

Next, loss-of-function and gain-of-function experiments were performed in TS cells (Fig. 3 *F–M*). Knockdown of KDM3A using specific shRNAs did not affect proliferation of TS cells in ambient or low oxygen tensions (Fig. S3*F*) but did inhibit low oxygen-activated TS cell differentiation-dependent movement through extracellular matrices and the activation of several low oxygen-responsive transcripts (*Mmp12, Il33, Ppp1r3*c, etc.; Fig. 3 *G–I*). Not all low oxygen/HIF dependent transcripts were responsive to KDM3A manipulation (Fig. S3*G*). In contrast to the knockdown experiments, ectopic expression of KDM3A activated some low oxygen-responsive transcripts (*Mmp12* and *Il33*) and stimulated movement of TS cells through extracellular matrices, both independent of exposure to low oxygen (Fig. 3 *J–M*). These gain-of-function actions were compromised in TS cells expressing a mutant KDM3A lacking demethylase activity (Fig. 3 *J–M*).

Because KDM3A acts as a histone H3K9 demethylase, we explored the H3K9 methylation landscape, including global- and gene-specific (*Mmp12*, *Il33*, and *Ppp1r3c*) H3K9 methylation in TS cells exposed to ambient or low oxygen conditions (Fig. 4). TS cells exposed to low oxygen and placentation sites exposed to maternal hypoxia exhibited generalized decreases in histone H3K9 monomethylation (H3K9-me1) and H3K9 dimethylation (H3K9-me2; Fig. S4 *A–C*). More specifically, low oxygen exposure led to significant decreases in histone H3K9 monomethylation (H3K9-me1) and H3K9 dimethylation (H3K9-me2) associated with regulatory regions of select hypoxia-HIF-KDM3A responsive genes but not control regions of the genome (Fig. 4 *B*, *G*, and *L* and Fig. S4 *E*, *H*, and *K*). Additionally, these shifts in H3K9 methylation status were not observed in KDM3A knockdown TS cells exposed to low oxygen (Fig. 4 *D*, *I*, and *N* and Fig. S4 *F* and *I*). Furthermore, KDM3A accumulated at these same putative regulatory regions associated with the *Mmp12*, *Il33*, and *Ppp1r3c* genes in low oxygen exposed TS cells (Fig. 4 *C*, *E*, *H*, *J*, *M*, and *O*) and at the *Mmp12* locus in hypoxia exposed gd 13.5 junctional zone tissue (Fig. S4*N*). Conserved hypoxia response element

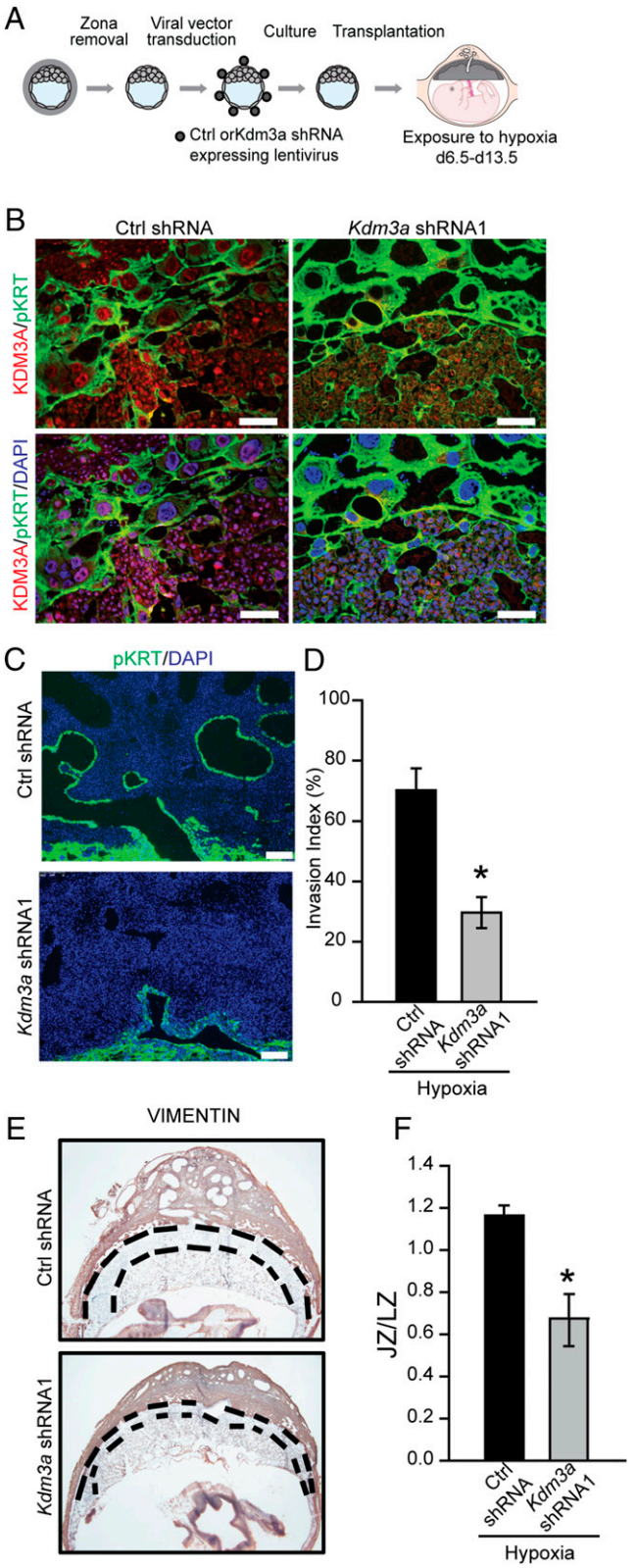

Fig. 7. KDM3A and hypoxia-activated trophoblast-directed uterine spiral artery remodeling. (*A*) Schematic showing experimental plan for lentiviral transduction of blastocysts and in vivo transfer to pseudopregnant recipient animals. (*B*) Representative images of immunolocalization of KDM3A and pan cytokeratin (pKRT) on gd 13.5 placentation sites expressing control (Ctrl) shRNA or *Kdm3a* shRNA exposed to 10.5% O_2 tension from gd 6.5 to 13.5. (*C*) Immunolocalization of pKRT on gd 13.5 placentation sites expressing Ctrl shRNA or *Kdm3a* shRNA exposed to 10.5% O_2 tension from gd 6.5 to 13.5. (*D*) Quantification of the depth of cytokeratin-positive cell penetration into the uterine mesometrial vasculature (n = 6/group; $^*P < 0.05$). (*E*) Localization of vimentin in placentation sites following Ctrl shRNA or *Kdm3a* shRNA transduction. (Scale bar, 1 mm.) Dashed black lines demarcate the location of the junctional zone (JZ) relative to the underlying labyrinth zone (LZ). (*F*) Ratio of cross-sectional areas of JZ vs. LZ from Ctrl shRNA and *Kdm3a* shRNA transduced placentation sites (n = 5/group; $^*P < 0.05$). Data presented in *D* and *F* were analyzed with Student *t* test.

(HRE) motifs could not be identified within the *Mmp12*, *Il33*, and *Ppp1r3c* regulatory regions binding KDM3A.

Thus far, the results supported a role for KDM3A as a mediator of hypoxia-HIF actions on trophoblast cells.

Conservation of Hypoxia-Dependent Responses in Human Trophoblast Cells. Next, we determined whether components of the hypoxia signaling pathway are conserved in human trophoblast cells (Fig. 5). First, we investigated responses of transformed trophoblast cell populations to low oxygen (Fig. 5 *A*–*C*). Each cell population responded to low oxygen with increases in *KDM3A*, *MMP12*, *IL33*, *PPP1R3C*, and *PLOD2* expression (Fig. 5 *A*–*C* and Fig. S5 *A*–*C*). Low oxygen conditions also stimulated the movement of trophoblast cells through extracellular matrices (Fig. 5 *D* and *E* and Fig. S5 *D* and *E*). These low oxygen-activated responses were disrupted in KDM3A knockdown human trophoblast cells. Low oxygen stimulated *KDM3A* expression in primary second trimester and term trophoblast cells, whereas low oxygen stimulated *MMP12* expression in primary second trimester trophoblasts but not primary term trophoblasts (Fig. 5*G*). The distribution of KDM3A transcripts and protein was also examined in the human placenta. KDM3A was localized to subpopulations of trophoblast cells within extravillous columns of first trimester human placentas, which represent the source of invasive trophoblast cells (Fig. 5*F* and Fig. S5 *F* and *G*). *MMP12* transcripts were also localized to the extravillous columns (Fig. 5*F* and Fig. S5*G*). Thus, a nexus between KDM3A and MMP12 was established in the developing human placenta.

KDM3A and MMP12 Expression in Diseased Human Placental Tissues. Preeclampsia is a multifaceted disease that can be associated with placental hypoxia and a failure of trophoblast-directed uterine spiral artery remodeling (3–5, 44–46). Analyses of placental tissue from preterm and term controls, intrauterine growth restriction, and preeclamptic pregnancies indicated that *KDM3A* expression was up-regulated in preeclampsia (Fig. 5*H* and Fig. S6*A*). This observation was further supported by quantitative RT-PCR (qRT-PCR) and Western blot analyses (Fig. 5 *J* and *K*). A finding consistent with the known hypoxia status of preeclamptic placental tissue (44–46) and the hypoxia-dependence of KDM3A expression (40–43). However, an up-regulation of *MMP12* did not accompany the up-regulation of *KDM3A* in placental tissues from preeclamptic pregnancies (Fig. 5 *H*–*K* and Fig. S6), in contrast to the coordinated expression of *KDM3A* and *MMP12* expression in first trimester placental tissue (Fig. 5*F* and Fig. S5*G*). A limitation of this experiment is that the analysis was performed on placental specimens obtained at delivery, whereas the hypoxia-HIF-KDM3A-MMP12 regulatory circuit we described is associated with an early pregnancy event. Nevertheless, the idea that MMP12 is dysregulated in preeclampsia is not unique to the present research; it is also supported by transcriptome profiling of chorionic villus samples (10–12 wk of gestation) from pregnancies destined to develop preeclampsia (47).

KDM3A and Hypoxia-Activated Trophoblast-Directed Uterine Spiral Artery Remodeling. The provocative findings supporting a conserved role for KDM3A in trophoblast cell responses to low oxygen prompted an in vivo assessment of its involvement in hypoxia-activated placental adaptations. A loss-of-function

strategy using lentiviral trophoblast-specific delivery of KDM3A shRNAs was used. Blastocysts were infected with KDM3A shRNAs or control shRNAs and examined ex vivo (Fig. 6*A*) or following transfer to pseudopregnant hosts (Fig. 7*A*). KDM3A shRNAs effectively down-regulated low oxygen-activated *Kdm3a* expression and in vitro blastocyst outgrowth (Fig. 6 *B*–*D*). Blastocyst outgrowth is a function of cell number, cell spreading, and cell movement, which were not distinguished in the assay. In vivo analysis demonstrated that KDM3A shRNAs down-regulated hypoxia-activated KDM3A expression (Fig. 7*B*) and interfered with hypoxia-activated trophoblast invasion and trophoblast-directed uterine spiral artery remodeling (Fig. 7*C*). Evidence also supported a role for KDM3A in hypoxia-induced expansion of the junctional zone (Fig. 7*D*). Our findings indicate that hypoxia acts through HIF and KDM3A to promote adaptations in placental development.

Discussion

During development, the hemochorial placenta is constructed in response to stimuli present in the maternal environment and optimized to facilitate nutrient delivery to the fetus. Plasticity in placental organization can be achieved via differential regulation of TS cell proliferation and differentiation. Among the myriad of potential signals emanating from the maternal environment, oxygen delivery plays a significant role. Eukaryotic cells have evolved mechanisms for adapting to low oxygen exposure (18). TS cells use hypoxia-signaling pathways to control placentation (15, 21–23, 48). The proximal response of TS cells to hypoxia is their differentiation into invasive trophoblast cells capable of targeting uterine spiral arteries and expanding nutrient flow to the placenta and fetus (14, 15). In the present report, hypoxia is shown to activate a HIF-KDM3A-MMP12 signaling cascade that promotes trophoblast invasion and trophoblast-directed uterine spiral artery remodeling.

TS cell adaptations to hypoxia are hierarchically regulated. Low oxygen exposure elicits a broad spectrum of changes in the TS cell transcriptome highlighted by activation of genes associated with cell movement, invasion, and vascular remodeling. A subset of the hypoxia-induced changes in gene expression is dependent on HIF signaling, especially those genes activated by hypoxia, and a more restricted cohort of the HIF-dependent genes is linked to the actions of KDM3A. Thus, a path can be constructed from hypoxia to HIF activation to increases in KDM3A expression to alterations in the histone methylation status of genes promoting development of the invasive trophoblast lineage.

Hypoxia, HIF, and KDM3A have been implicated in regulating epithelial mesenchymal transition and cell invasion in disease states, including cancers (18, 25, 26, 42, 43). HIF binds to HREs at the *Kdm3a* locus and stimulates *Kdm3a* transcription (42, 43). KDM3A targets histone H3K9me1 and H3K9me2 for demethylation and thus extends and amplifies HIF signaling (42, 43). Early events in the development of the trophoblast lineage have also been associated with the methylation status of histone H3K9 (49). The histone H3K9me2 mark is associated with gene repression, and thus its removal is linked to gene activation (50). Loss of histone H3K9me2 modifications at several loci corresponding to hypoxia-HIF-KDM3A targets correlate with increases in target gene expression. Effectively, KDM3A regulates key downstream events in the development of the invasive trophoblast lineage and especially those necessary for trophoblast-directed uterine spiral artery remodeling, representing critical adaptations at the placentation site.

KDM3A is specifically targeted to its sites of action within the genome. HIF1A can recruit KDM3A to some of its target genes, including the *Glut3* locus, resulting in H3K9me2 demethylation and transcriptional up-regulation (43). Under hypoxic conditions in TS cells, KDM3A may be delivered by HIF transcription factors to its target genes in some instances, whereas arrival at other loci may be independent of HIF (*Mmp12* and *Il33*). This conclusion is based on the observed differential outcomes of loss-of-function and gain-of-function KDM3A manipulations in TS cells and the absence of conserved HIF binding motifs in regulatory regions binding KDM3A. In addition to HIF, there is evidence for other types of transcription factors (e.g., nuclear receptors and OCT1) guiding KDM3A to its genomic targets in various nontrophoblast cells (51–53). Mechanisms controlling KDM3A arrival at its target loci within the TS cell genome are yet to be elucidated.

Among the hypoxia-HIF-KDM3A targets in trophoblast cells, we focused our attention on MMP12 as a downstream effector. MMP12 was shown to be essential for placental adaptations to hypoxia, where it promoted endovascular invasion of trophoblast cells. These adaptive responses and actions of MMP12 are conserved (30, 34). Trophoblast-derived MMP12 contributes to uterine spiral artery remodeling in the human (30, 34). MMP12 acts on trophoblast cell invasive behavior in a cell autonomous mode. *Mmp12*-null TS cells exhibited disruptions in invasion, an observation reminiscent of defective invasive properties associated with MMP12 deficient macrophages (35), and consistent with in vivo findings presented in this report. Even though *Mmp12*-null TS cells did not invade through an extracellular matrix in response to low oxygen, some other cellular responses were consistent with the abilities of the mutant TS cells to respond to low oxygen. However, unlike WT TS cells, a down-regulation of *Cdh1* in response to low oxygen was not observed. CDH1 encodes a protein pivotal to epithelial cell–cell adhesion and in general opposes invasive behaviors accompany cell invasion (54, 55), Previously, Aplin and colleagues provided compelling evidence that elastin-derived peptides promote human trophoblast cell migration and invasion (56). Thus, an MMP12 product of elastin degradation or MMP12-dependent actions on other cellular/extracellular substrate(s) could represent the active factor driving trophoblast migration and endovascular invasion critical to hypoxia-activated placental adaptations in the rat. Although MMP12 is vital to hypoxia activated trophoblast invasion, it is dispensable for interstitial and endovascular trophoblast invasion during the last week of gestation in the rat. These latter events may be influenced by the actions of other MMPs possessing substrate specificities that overlap with MMP12.

In conclusion, our observations connect hypoxia-dependent establishment of the invasive trophoblast lineage to HIF, KDM3A, and MMP12. HIF signaling is a key regulator of KDM3A expression. KDM3A acts on the epigenetic landscape of target loci, including the *Mmp12* gene. MMP12 is a critical downstream effector of hypoxia-HIF-KDM3A signaling, controlling trophoblast invasion and trophoblast-directed uterine spiral artery remodeling. The hypoxia-HIF-KDM3A-MMP12 regulatory pathway is conserved and facilitates placental adaptations to environmental challenges. Interruption of the hypoxia-HIF-KDM3A-MMP12 signaling cascade may be at the origin of some placental diseases.

Methods

The University of Kansas Medical Center Animal Care and Use Committee approved all protocols performed. Animals and tissue collection, rat TS and human trophoblast cell cultures, DNA microarray, RT-PCR, immunohistochemistry, in situ hybridization, morphometric measurements, Western blot analysis, generation of the *Mmp12* mutant rat model, shRNA constructs and production of lentivirus, ectopic expression of KDM3A, Matrigel invasion assay, chromatin immunoprecipitation analysis, ex vivo lentiviral trophoblast shRNA delivery and analyses, and statistical analyses are provided in *SI Methods* and primer and shRNA sequences are provided in Tables S2–S4.

ACKNOWLEDGMENTS. We thank Dr. Khursheed Iqbal for providing valuable feedback and suggestions during the course of the research, Dr. Christopher Mack (University of North Carolina) for providing a Kdm3a expression vector, Dr. Sumedha S. Gunewardena for assistance with the bioinformatic analysis, Mr. Clark Bloomer for assistance with the DNA microarray analysis, and Stacy McClure for administrative assistance. This work was supported by NIH Grants HD020676 and HD079363. G.X.R. was supported by a postdoctoral fellowship from the American Heart Association.

1. Georgiades P, Ferguson-Smith AC, Burton GJ (2002) Comparative developmental anatomy of the murine and human definitive placentae. *Placenta* 23(1):3–19.
2. Harris LK (2010) Review: Trophoblast-vascular cell interactions in early pregnancy: How to remodel a vessel. *Placenta* 31(Suppl):S93–S98.
3. Maltepe E, Fisher SJ (2015) Placenta: The forgotten organ. *Annu Rev Cell Dev Biol* 31: 523–552.
4. Kaufmann P, Black S, Huppertz B (2003) Endovascular trophoblast invasion: implications for the pathogenesis of intrauterine growth retardation and preeclampsia. *Biol Reprod* 69(1):1–7.
5. Pijnenborg R, Vercruysse L, Hanssens M (2006) The uterine spiral arteries in human pregnancy: Facts and controversies. *Placenta* 27(9-10):939–958.
6. Soares MJ, Chakraborty D, Kubota K, Renaud SJ, Rumi MA (2014) Adaptive mechanisms controlling uterine spiral artery remodeling during the establishment of pregnancy. *Int J Dev Biol* 58(2-4):247–259.
7. Damsky CH, Fisher SJ (1998) Trophoblast pseudo-vasculogenesis: Faking it with endothelial adhesion receptors. *Curr Opin Cell Biol* 10(5):660–666.
8. Rai A, Cross JC (2014) Development of the hemochorial maternal vascular spaces in the placenta through endothelial and vasculogenic mimicry. *Dev Biol* 387(2):131–141.
9. Pijnenborg R, Robertson WB, Brosens I, Dixon G (1981) Review article: Trophoblast invasion and the establishment of haemochorial placentation in man and laboratory animals. *Placenta* 2(1):71–91.
10. Pijnenborg R, Vercruysse L (2010) Animal models of deep trophoblast invasion. *Placental Bed Disorders: Basic Science and Its Translation to Obstetrics*, eds Pijnenborg R, Brosens I, Romero R (Cambridge Univ Press, Cambridge, UK), pp 127–139.
11. Soares MJ, Chakraborty D, Karim Rumi MA, Konno T, Renaud SJ (2012) Rat placentation: An experimental model for investigating the hemochorial maternal-fetal interface. *Placenta* 33(4):233–243.
12. Myatt L (2006) Placental adaptive responses and fetal programming. *J Physiol* 572(Pt 1):25–30.
13. Kadyrov M, Schmitz C, Black S, Kaufmann P, Huppertz B (2003) Pre-eclampsia and maternal anaemia display reduced apoptosis and opposite invasive phenotypes of extravillous trophoblast. *Placenta* 24(5):540–548.
14. Rosario GX, Konno T, Soares MJ (2008) Maternal hypoxia activates endovascular trophoblast cell invasion. *Dev Biol* 314(2):362–375.
15. Chakraborty D, Rumi MA, Konno T, Soares MJ (2011) Natural killer cells direct hemochorial placentation by regulating hypoxia-inducible factor dependent trophoblast lineage decisions. *Proc Natl Acad Sci USA* 108(39):16295–16300.
16. Zhou Y, et al. (1993) Increased depth of trophoblast invasion after chronic constriction of the lower aorta in rhesus monkeys. *Am J Obstet Gynecol* 169(1):224–229.
17. Dunwoodie SL (2009) The role of hypoxia in development of the Mammalian embryo. *Dev Cell* 17(6):755–773.
18. Semenza GL (2010) Oxygen homeostasis. *Wiley Interdiscip Rev Syst Biol Med* 2(3): 336–361.
19. Gnarra JR, et al. (1997) Defective placental vasculogenesis causes embryonic lethality in VHL-deficient mice. *Proc Natl Acad Sci USA* 94(17):9102–9107.
20. Kozak KR, Abbott B, Hankinson O (1997) ARNT-deficient mice and placental differentiation. *Dev Biol* 191(2):297–305.
21. Adelman DM, Gertsenstein M, Nagy A, Simon MC, Maltepe E (2000) Placental cell fates are regulated *in vivo* by HIF-mediated hypoxia responses. *Genes Dev* 14(24): 3191–3203.
22. Cowden Dahl KD, et al. (2005) Hypoxia-inducible factors 1alpha and 2alpha regulate trophoblast differentiation. *Mol Cell Biol* 25(23):10479–10491.
23. Maltepe E, et al. (2005) Hypoxia-inducible factor-dependent histone deacetylase activity determines stem cell fate in the placenta. *Development* 132(15):3393–3403.
24. Takeda K, et al. (2006) Placental but not heart defects are associated with elevated hypoxia-inducible factor alpha levels in mice lacking prolyl hydroxylase domain protein 2. *Mol Cell Biol* 26(22):8336–8346.
25. Melvin A, Rocha S (2012) Chromatin as an oxygen sensor and active player in the hypoxia response. *Cell Signal* 24(1):35–43.
26. Hancock RL, Dunne K, Walport LJ, Flashman E, Kawamura A (2015) Epigenetic regulation by histone demethylases in hypoxia. *Epigenomics* 7(5):791–811.
27. Page-McCaw A, Ewald AJ, Werb Z (2007) Matrix metalloproteinases and the regulation of tissue remodelling. *Nat Rev Mol Cell Biol* 8(3):221–233.
28. Kessenbrock K, Plaks V, Werb Z (2010) Matrix metalloproteinases: Regulators of the tumor microenvironment. *Cell* 141(1):52–67.
29. Solberg H, Rinkenberger J, Danø K, Werb Z, Lund LR (2003) A functional overlap of plasminogen and MMPs regulates vascularization during placental development. *Development* 130(18):4439–4450.
30. Harris LK, et al. (2010) Trophoblast- and vascular smooth muscle cell-derived MMP-12 mediates elastolysis during uterine spiral artery remodeling. *Am J Pathol* 177(4): 2103–2115.
31. Plaks V, et al. (2013) Matrix metalloproteinase-9 deficiency phenocopies features of preeclampsia and intrauterine growth restriction. *Proc Natl Acad Sci USA* 110(27): 11109–11114.
32. Asanoma K, et al. (2011) FGF4-dependent stem cells derived from rat blastocysts differentiate along the trophoblast lineage. *Dev Biol* 351(1):110–119.
33. Ain R, Canham LN, Soares MJ (2003) Gestation stage-dependent intrauterine trophoblast cell invasion in the rat and mouse: Novel endocrine phenotype and regulation. *Dev Biol* 260(1):176–190.
34. Harris LK, et al. (2007) BeWo cells stimulate smooth muscle cell apoptosis and elastin breakdown in a model of spiral artery transformation. *Hum Reprod* 22(11): 2834–2841.
35. Shipley JM, Wesselschmidt RL, Kobayashi DK, Ley TJ, Shapiro SD (1996) Metalloelastase is required for macrophage-mediated proteolysis and matrix invasion in mice. *Proc Natl Acad Sci USA* 93(9):3942–3946.
36. Benita Y, et al. (2009) An integrative genomics approach identifies Hypoxia Inducible Factor-1 (HIF-1)-target genes that form the core response to hypoxia. *Nucleic Acids Res* 37(14):4587–4602.
37. Mole DR, et al. (2009) Genome-wide association of hypoxia-inducible factor (HIF)-1α and HIF-2α DNA binding with expression profiling of hypoxia-inducible transcripts. *J Biol Chem* 284(25):16767–16775.
38. Xia X, et al. (2009) Integrative analysis of HIF binding and transactivation reveals its role in maintaining histone methylation homeostasis. *Proc Natl Acad Sci USA* 106(11): 4260–4265.
39. Schödel J, et al. (2011) High-resolution genome-wide mapping of HIF-binding sites by ChIP-seq. *Blood* 117(23):e207–e217.
40. Beyer S, Kristensen MM, Jensen KS, Johansen JV, Staller P (2008) The histone demethylases JMJD1A and JMJD2B are transcriptional targets of hypoxia-inducible factor HIF. *J Biol Chem* 283(52):36542–36552.
41. Pollard PJ, et al. (2008) Regulation of Jumonji-domain-containing histone demethylases by hypoxia-inducible factor (HIF)-1alpha. *Biochem J* 416(3):387–394.
42. Krieg AJ, et al. (2010) Regulation of the histone demethylase JMJD1A by hypoxia-inducible factor 1 alpha enhances hypoxic gene expression and tumor growth. *Mol Cell Biol* 30(1):344–353.
43. Mimura I, et al. (2012) Dynamic change of chromatin conformation in response to hypoxia enhances the expression of GLUT3 (SLC2A3) by cooperative interaction of hypoxia-inducible factor 1 and KDM3A. *Mol Cell Biol* 32(15):3018–3032.
44. Caniggia I, Grisaru-Gravnosky S, Kuliszewsky M, Post M, Lye SJ (1999) Inhibition of TGF-beta 3 restores the invasive capability of extravillous trophoblasts in preeclamptic pregnancies. *J Clin Invest* 103(12):1641–1650.
45. Rajakumar A, Brandon HM, Daftary A, Ness R, Conrad KP (2004) Evidence for the functional activity of hypoxia-inducible transcription factors overexpressed in preeclamptic placentae. *Placenta* 25(10):763–769.
46. Tal R (2012) The role of hypoxia and hypoxia-inducible factor-1alpha in preeclampsia pathogenesis. *Biol Reprod* 87(6):134.
47. Founds SA, et al. (2009) Altered global gene expression in first trimester placentas of women destined to develop preeclampsia. *Placenta* 30(1):15–24.
48. Zhou S, Xie Y, Puscheck EE, Rappolee DA (2011) Oxygen levels that optimize TSC culture are identified by maximizing growth rates and minimizing stress. *Placenta* 32(6):475–481.
49. Rugg-Gunn PJ, Cox BJ, Ralston A, Rossant J (2010) Distinct histone modifications in stem cell lines and tissue lineages from the early mouse embryo. *Proc Natl Acad Sci USA* 107(24):10783–10790.
50. Greer EL, Shi Y (2012) Histone methylation: A dynamic mark in health, disease and inheritance. *Nat Rev Genet* 13(5):343–357.
51. Yamane K, et al. (2006) JHDM2A, a JmjC-containing H3K9 demethylase, facilitates transcription activation by androgen receptor. *Cell* 125(3):483–495.
52. Shakya A, Kang J, Chumley J, Williams MA, Tantin D (2011) Oct1 is a switchable, bipotential stabilizer of repressed and inducible transcriptional states. *J Biol Chem* 286(1):450–459.
53. Abe Y, et al. (2015) JMJD1A is a signal-sensing scaffold that regulates acute chromatin dynamics via SWI/SNF association for thermogenesis. *Nat Commun* 6:7052.
54. Harris LK, Jones CJ, Aplin JD (2009) Adhesion molecules in human trophoblast: A review. II. extravillous trophoblast. *Placenta* 30(4):299–304.
55. Schneider MR, Kolligs FT (2015) E-cadherin's role in development, tissue homeostasis and disease: Insights from mouse models: Tissue-specific inactivation of the adhesion protein E-cadherin in mice reveals its functions in health and disease. *BioEssays* 37(3): 294–304.
56. Desforges M, Harris LK, Aplin JD (2015) Elastin-derived peptides stimulate trophoblast migration and invasion: A positive feedback loop to enhance spiral artery remodelling. *Mol Hum Reprod* 21(1):95–104.
57. Ain R, Konno T, Canham LN, Soares MJ (2006) Phenotypic analysis of the rat placenta. *Methods Mol Med* 121:295–313.
58. Tanaka S, Kunath T, Hadjantonakis AK, Nagy A, Rossant J (1998) Promotion of trophoblast stem cell proliferation by FGF4. *Science* 282(5396):2072–2075.
59. Faria TN, Soares MJ (1991) Trophoblast cell differentiation: Establishment, characterization, and modulation of a rat trophoblast cell line expressing members of the placental prolactin family. *Endocrinology* 129(6):2895–2906.
60. Clapcote SJ, Roder JC (2005) Simplex PCR assay for sex determination in mice. *Biotechniques* 38(5):702–706, 704, 706.
61. Kliman HJ, Nestler JE, Sermasi E, Sanger JM, Strauss JF, 3rd (1986) Purification, characterization, and in vitro differentiation of cytotrophoblasts from human term placentae. *Endocrinology* 118(4):1567–1582.
62. Kuroki S, et al. (2013) Epigenetic regulation of mouse sex determination by the histone demethylase Jmjd1a. *Science* 341(6150):1106–1109.
63. Lee DS, Rumi MA, Konno T, Soares MJ (2009) *In vivo* genetic manipulation of the rat trophoblast cell lineage using lentiviral vector delivery. *Genesis* 47(7):433–439.
64. Lockman K, Taylor JM, Mack CP (2007) The histone demethylase, Jmjd1a, interacts with the myocardin factors to regulate SMC differentiation marker gene expression. *Circ Res* 101(12):e115–e123.